



Article

Extending the Toolkit for Beauty: Differential Co-Expression of *DROOPING LEAF*-Like and Class B MADS-Box Genes during *Phalaenopsis* Flower Development

Francesca Lucibelli ¹, Maria Carmen Valoroso ¹, Günter Theißen ², Susanne Nolden ², Mariana Mondragon-Palomino ^{3,*} and Serena Aceto ^{1,*}

¹ Department of Biology, University of Naples Federico II, 80126 Napoli, Italy; francesca.lucibelli@unina.it (F.L.); mariacarmen.valoroso@unina.it (M.C.V.)

² Matthias Schleiden Institute/Genetics, Friedrich Schiller University Jena, 07743 Jena, Germany; guenter.theissen@uni-jena.de (G.T.); nolden_susanne@yahoo.de (S.N.)

³ Department of Cell Biology and Plant Biochemistry, University of Regensburg, 93040 Regensburg, Germany

* Correspondence: serena.aceto@unina.it (S.A.); mariana.mondragon@biomax.com (M.M.-P.)

[†] Current address: Biomax Informatics AG, 82152 Planegg, Germany.

Citation: Lucibelli, F.; Valoroso, M.C.; Theißen, G.; Nolden, S.; Mondragon-Palomino, M.; Aceto, S. Extending the Toolkit for Beauty: Differential Co-Expression of *DROOPING LEAF*-Like and Class B MADS-Box Genes during *Phalaenopsis* Flower Development. *Int. J. Mol. Sci.* **2021**, *22*, 7025. <https://doi.org/10.3390/ijms22137025>

Academic Editor: Pedro Martínez-Gómez

Received: 3 June 2021

Accepted: 27 June 2021

Published: 29 June 2021

Publisher's Note: MDPI stays neutral with regard to jurisdictional claims in published maps and institutional affiliations.



Copyright: © 2021 by the authors. Licensee MDPI, Basel, Switzerland. This article is an open access article distributed under the terms and conditions of the Creative Commons Attribution (CC BY) license (<http://creativecommons.org/licenses/by/4.0/>).

Abstract: The molecular basis of orchid flower development is accomplished through a specific regulatory program in which the class B MADS-box *AP3/DEF* genes play a central role. In particular, the differential expression of four class B *AP3/DEF* genes is responsible for specification of organ identities in the orchid perianth. Other MADS-box genes (*AGL6* and *SEP*-like) enrich the molecular program underpinning the orchid perianth development, resulting in the expansion of the original “orchid code” in an even more complex gene regulatory network. To identify candidates that could interact with the *AP3/DEF* genes in orchids, we conducted an *in silico* differential expression analysis in wild-type and peloric *Phalaenopsis*. The results suggest that a YABBY *DL*-like gene could be involved in the molecular program leading to the development of the orchid perianth, particularly the labellum. Two YABBY *DL/CRC* homologs are present in the genome of *Phalaenopsis equestris*, *PeDL1* and *PeDL2*, and both express two alternative isoforms. Quantitative real-time PCR analyses revealed that both genes are expressed in column and ovary. In addition, *PeDL2* is more strongly expressed the labellum than in the other tepals of wild-type flowers. This pattern is similar to that of the *AP3/DEF* genes *PeMADS3/4* and opposite to that of *PeMADS2/5*. In peloric mutant *Phalaenopsis*, where labellum-like structures substitute the lateral inner tepals, *PeDL2* is expressed at similar levels of the *PeMADS2-5* genes, suggesting the involvement of *PeDL2* in the development of the labellum, together with the *PeMADS2-PeMADS5* genes. Although the yeast two-hybrid analysis did not reveal the ability of *PeDL2* to bind the *PeMADS2-PeMADS5* proteins directly, the existence of regulatory interactions is suggested by the presence of CARG-boxes and other MADS-box transcription factor binding sites within the putative promoter of the orchid *DL2* gene.

Keywords: *DROOPING LEAF*; flower development; gene expression; Orchidaceae; YABBY transcription factors

1. Introduction

The Orchidaceae is one of the widely distributed and most diversified families of angiosperms. Their evolutionary success is possibly due to sundry causes such as epiphytism, extraordinary adaptive capacities to different habitats, highly specialized pollination strategies, and diversified flower morphology [1–3]. Despite the diversity of flower colors, sizes, shapes, and appendages, the floral organs of orchids share a common organization (Figure 1). There are three outer tepals in the first floral whorl; in the second whorl, the three tepals are distinguished into two lateral inner tepals and a median inner

tepals called lip or labellum. This organ often has a peculiar morphology and bears distinct color patterns (Figure 1a,b). Female and male reproductive organs are fused to form the gynostemium or column, at whose apex are located the pollinia. The ovary is placed at the base of the gynostemium, and its development is activated by pollination [4].

The labellum is a central organ in orchid pollination because of its strikingly distinct morphology and its direct opposition to the gynostemium. Therefore, its showy color patterns and structures are visual attractants and it act as a landing platform that guides pollinators towards the gynostemium. Because the labellum is the uppermost perianth organ, its role in pollination depends on becoming the lowermost through resupination, a 180° developmental rotation of the flower pedicel or ovary (Figure 1a) [5].

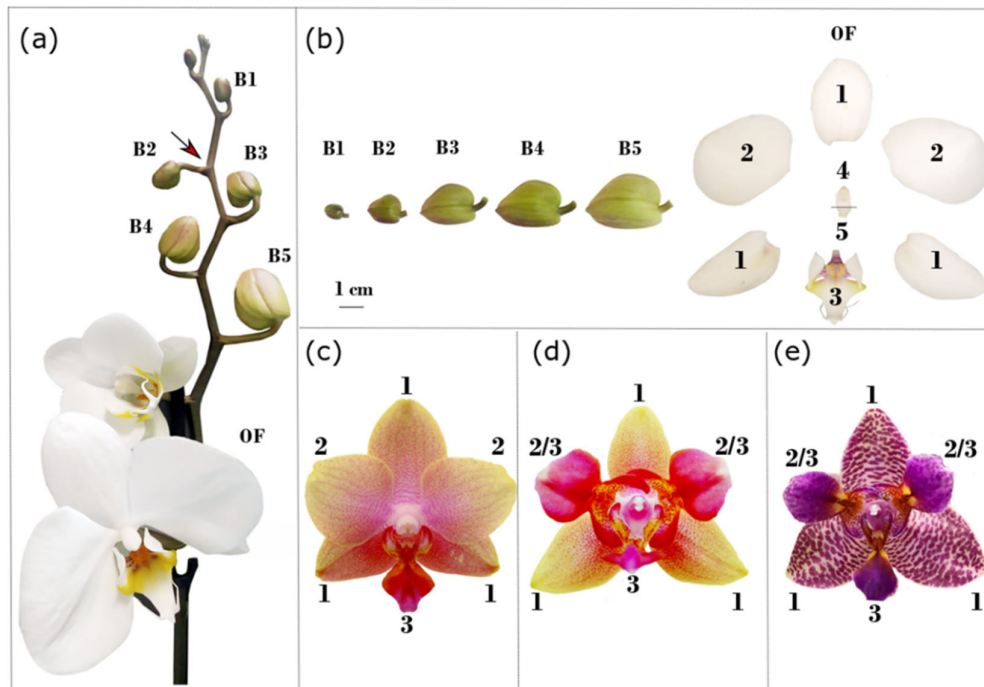


Figure 1. Wild-type and peloric mutants of *Phalaenopsis*. (a) Wild-type *P. aphrodite*; (b) floral buds at stages B1–B5 and floral organs at the OF stage of the wild-type *P. aphrodite*; (c) flower of the wild-type *Phalaenopsis* hybrid “Athens”; (d) flower of the peloric mutant *Phalaenopsis* hybrid “Athens”; (e) flower of the peloric mutant *Phalaenopsis* hybrid “Joy Fairy Tale”. The arrow in (a) indicates the point of rotation of the pedicel during resupination. Size of the developmental stages: B1 (0.5–1 cm), B2 (1–1.5 cm), B3 (1.5–2 cm), B4 (2–2.5 cm), B5 (2.5–3 cm), OF (open flower). 1, outer tepals; 2, lateral inner tepals; 3, labellum; 4, column; 5, ovary; 2/3, labellum-like organs.

Bilateral symmetry or zygomorphy in orchids is a syndrome defined by the association of several characters (e.g., labellum and the developmental suppression of adaxial stamens). This association took place early in Orchidaceae evolution and became the basis for the progressive addition of further innovations like pollinaria, a spur, or showy markings on the labellum [4]. The concurrence of these floral features is considered a key morphological innovation in the two most derived and diverse orchid subfamilies Epidendroideae and Orchidoideae [4]. Together they mediate the specialized relationships of this family with pollinators, facilitating the processes of prezygotic reproductive isolation [6,7].

Because of the central role of the labellum in orchid reproduction, its developmental origin is a subject of intense study [4,8–10]. In the last decade, several gene regulatory models inspired by the more general angiosperm ABC model [11,12] helped to explain the developmental specification of the distinct orchid perianth organs [13–18]. Specifically, the “orchid code” argues that the diversification of the organs of the orchid

perianth is due to the combined differential expression of class B MADS-box genes belonging to the *AP3/DEF* group [13–15]. The “homeotic orchid tepals” (HOT model) proposes a combinatorial action of homeotic MADS-box proteins consistent with the “orchid code” [16]. The more recent “P-code” model hypothesizes a pivotal role of the class B and *AGL6* MADS-box genes in forming the orchid perianth [19].

In order to understand the more extensive regulatory network behind orchid flower development, we and others have found that, like *AP3/DEFs*, also candidate *SEP*-, *FUL*-, *AG*-, and *STK*-like MADS-box genes have been duplicated in the Orchidaceae. However, only some of them are differentially expressed in association with the distinct flower organs. For instance, in developing *Phalaenopsis* flowers, we observed that *SEP3*-like and *DEF*-like genes have common expression domains. This shared domain of expression suggests that both candidates are associated with labellum specification, and that similar positional cues determine their expression domains [20]. Elucidating the nature of the positional cues behind the development of specific orchid flower organs is a central question to understand the developmental program of this family.

Top candidates for providing the positional information for differentially expressed MADS-box genes are CYCLOIDEA-like (CYC-like) transcription factors [13], which are well known for their role in flower bilateral symmetry specification in core eudicots [21–25]. Comparative studies of CYC-like genes identified several major, well-supported monocot-specific clades and reported the first CYC-like genes in orchid species [26–28]. Additional studies also showed that the DDR regulatory module composed of the MYB factors *DIVARICATA*, *DRIF*, and *RADIALIS*, responsible in *Antirrhinum majus* for bilateral flower symmetry [29,30], seems to be conserved in orchids [31–33]. However, the critical CYC-like transcription factor that activates the transcription of *RADIALIS* in *A. majus* [21,34] is not conserved in orchids. Moreover, the current literature reports contrasting results [26–28,35], possibly because the functional equivalent of CYC, if it exists, has not yet been identified in orchids.

Our interest in identifying additional components of the regulatory network determining orchid flower organ identity prompted us to conduct a preliminary in silico differential expression study using RNA-seq data of *Phalaenopsis*. This preliminary work suggests a scenario where MADS-box genes and members of the plant-specific family of transcription factors termed YABBY contribute to labellum development.

During the course of angiosperm evolution, the YABBY *DROOPING LEAF/CRABS CLAW (DL/CRC)* genes came to regulate the development of different structures like the carpel, nectaries, or the leaf mid-rib [36]. In addition, *DL/CRC* and other members of the YABBY gene family like *FILAMENTOUS FLOWER (FIL)* [37,38] respectively determine flower meristem and organ identity in *Arabidopsis* and rice [37,38]. In the rice flower meristem, the expression domain of *DL* is delimited by the class B MADS-box gene *SUPERWOMAN1* [37,39], thus suggesting a regulatory relationship between them. Additional evidence of regulatory interaction between *DL/CRC* and MADS-box genes comes from maize. In this species, the co-orthologs *drl1* and *drl2* have a potential antagonistic relationship with *silky1*, the ortholog of the class B *APETALA3/DEFICIENS* gene, during floral patterning and establishment of floral bilateral symmetry [40].

The existence of a regulatory relationship between *DL/CRC* and MADS-box genes in model dicot and monocot species inspired us to explore the role of *DL*-like genes in orchids. In this family, gene duplication and differential expression of *DEF*-like class B MADS-box genes play a pivotal role in modularizing the perianth [13–19,41,42]. However, it is not yet clear as to which positional cues determine their expression domains, resulting in flower bilateral symmetry. The present study tests the hypothesis that *DL*-like orchid genes are associated with the development of distinct orchid flower organs. To this purpose, we compared their patterns of expression with those of *DEFICIENS*-like MADS-box genes *PeMADS2*, *PeMADS3*, *PeMAD4*, and *PeMADS5* (*PeMADS2*–*PeMADS5*) in wild-type and peloric *Phalaenopsis* flowers. These mutants have labellum-like structures that substitute the lateral inner tepals, thus lacking the bilateral symmetry of the perianth, and

are especially useful to study genes possibly involved in orchid perianth formation. Next, we tested whether the co-expression of *DL*-like and *DEF*-like genes also involves direct protein–protein interactions via yeast two-hybrid assays. Finally, we scanned the putative promoters of the *DL*-like genes of *Phalaenopsis* and *Dendrobium* to identify conserved motifs with possible regulatory functions.

2. Results

2.1. Identification of Transcription Factors Differentially Expressed in the Labellum

Our initial RNA-seq screening of the *Phalaenopsis* hyb. “Athens” (Figure 1c,d) inner-perianth transcriptome showed over 78% of the read pairs mapped to the *Phalaenopsis equestris* genome v 1.0 [43]. About 68% of the transcripts annotated (21,200 genes) are expressed in the flower organs analyzed with at least 1 TPM (transcripts per kilobase million). Labellum-like lateral inner tepals of peloric flowers and wild-type labella share 98% of all expressed genes. This indicates that these organs express almost the same genes, strongly suggesting that they have the same organ identity (Supplementary Figure S1a).

Analyses of differential gene expression yielded an interesting group of transcripts significantly up- or downregulated in wild-type lateral inner tepals compared to the labellum (Supplementary Figure S1b and Data S1). Among them, we identified transcripts that are possibly associated with labellum development, encoding DROOPING LEAF-like proteins (*DL*-like) and the class B MADS-domain protein PeMADS2 (Supplementary Figure S1c). In our analysis, two *DL*-like transcripts are downregulated in wild-type lateral inner tepals, in comparison to their wild-type and peloric labella levels. Transcripts of class B MADS-box gene PeMADS2 are upregulated in wild-type lateral inner tepals, just as documented by qPCR in the “orchid code” [13–15]. Furthermore, *CYC-TB1*-like genes are expressed in lateral inner tepals and labellum at levels under 1 TPM. This extremely low level of expression of *CYC-TB1*-like genes during orchid development has also been observed in previous studies [26].

We then conducted an *in silico* differential expression analysis using publicly available reads of the perianth organs of wild-type and peloric mutant *Phalaenopsis* hyb. “Brother Spring Dancer” KHM190 [44]. We mapped and quantified the reads against the transcriptome of *Phalaenopsis* hyb. “Brother Spring Dancer” assembled from the Illumina raw reads. In this case we also found transcripts encoding class B MADS-box proteins differentially expressed among the organs of the wild-type plant, and detected differential expression for a transcript encoding a *DL*-like protein (Supplementary Data S2). In particular, in the wild-type *Phalaenopsis* this *DL*-like transcript showed a 3 to 4 log₂FC expression in labellum than in lateral inner tepals. No significant difference was observed between the transcripts of this gene in the labellum and labellum-like lateral inner tepals of the peloric mutant *Phalaenopsis* hyb. “Brother Spring Dancer” (Supplementary Data S2).

The differential pattern of expression of the *DL*-like transcript is analogous to those observed in MADS-box *DEF*-like genes *PeMADS3* and *PeMADS4*, which are highly expressed in the wild-type labellum and labellum-like structures of peloric mutants [14,45]. This similarity suggests an association between the activity of *DL*-like and *DEF*-like homeotic genes and the development of the labellum.

Further *in silico* analyses of the reference transcriptome of *Phalaenopsis* hyb. “Brother Spring Dancer” identified two *DL*-like transcripts, *PeDL1* and *PeDL2*, each with two different isoforms.

We confirmed the presence of these transcripts by the PCR amplification of cDNA from perianth tissues of *Phalaenopsis* hyb. “Athens” followed by cloning and sequencing, and deposited the sequences in GenBank with the accession numbers MW574592, MW574593 (*PeDL1_1* and *PeDL1_2*), MW574594, and MW574595 (*PeDL2_1* and *PeDL2_2*). The longest isoforms of both transcripts (*PeDL1_1* and *PeDL2_1*) encode proteins containing a C2C2 zinc-finger domain at the N-terminus and a YABBY domain, whereas both the alternative isoforms encode proteins missing the C2C2 zinc-finger domain completely

(*PeDL1_2*) or partially (*PeDL2_2*) (Supplementary Figure S2). The *PeDL1_1* (189 aa) and *PeDL2_1* (196 aa) proteins are 64.3% similar, with highly conserved YABBY domains and more variable C2C2 zinc-finger domains. In comparison, the region spanning from the C2C2 to the YABBY domain and the C-terminal region are the less-conserved parts of these proteins (Supplementary Figure S2).

2.2. Genomic Organization of the *PeDL1* and *PeDL2* Genes

Reconstruction of the genomic organization of the *PeDL1* and *PeDL2* genes based on BLAST analyses of the longest *PeDL* transcripts against the assembled genome of *Phalaenopsis equestris* [43] showed the *PeDL* genes have seven exons and six introns (Figure 2). The large intron 4 is particularly rich in repetitive sequences. This feature has affected the correct assembly of the *PeDL1* and *PeDL2* genes, which were both split in two different genomic scaffolds (Scaffold000404_23 and Scaffold000404_21 for *PeDL1*; Scaffold000061_46 and Scaffold000061_45 for *PeDL2*).

The alignment of the short transcripts *PeDL1_2* and *PeDL2_2* with the corresponding genomic region revealed the presence of a putative alternative transcription start site within intron 1 of *PeDL2* and intron 2 of *PeDL1*, resulting in transcripts whose ATG start codon is located within exon 2 and exon 3, respectively (Figure 2).

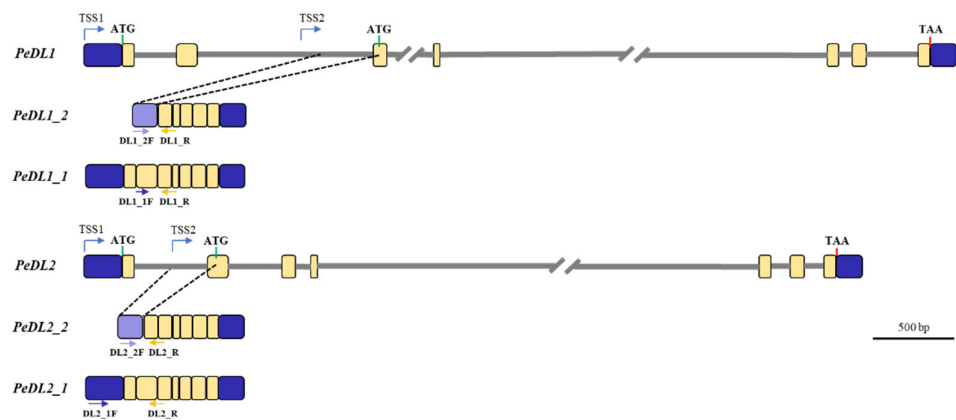


Figure 2. Genomic organization of the *PeDL1* and *PeDL2* transcribed regions of *P. equestris* and diagram of the corresponding alternative transcripts. The blue boxes represent the 5'- and 3'-UTRs; the yellow boxes represent the coding regions, the gray lines represent the introns. Introns of unknown size are shown as interrupted gray lines. The green and red bars indicate the position of the translation start (ATG) and stop (TAA) codons, respectively. TSS1 and 2 are the putative alternative transcription start sites of the different isoforms. The blue and yellow arrows indicate the position of the isoform-specific primer pairs.

2.3. Differential Expression of the *PeDL1* and *PeDL2* Genes

To analyze the expression pattern of *PeDL1* and *PeDL2* in the floral organs of *Phalaenopsis*, we performed quantitative real-time PCR on cDNA from different organs of the wild-type *Phalaenopsis* hyb. “Athens” dissected from floral buds of ~1 cm (B2 stage, Figure 1c). Both genes are highly expressed in the column and ovary. However, the *PeDL2* isoforms are also highly expressed in the labellum relative to outer and the other inner tepals. These results confirm the initial in silico differential expression analysis (Figure 3).

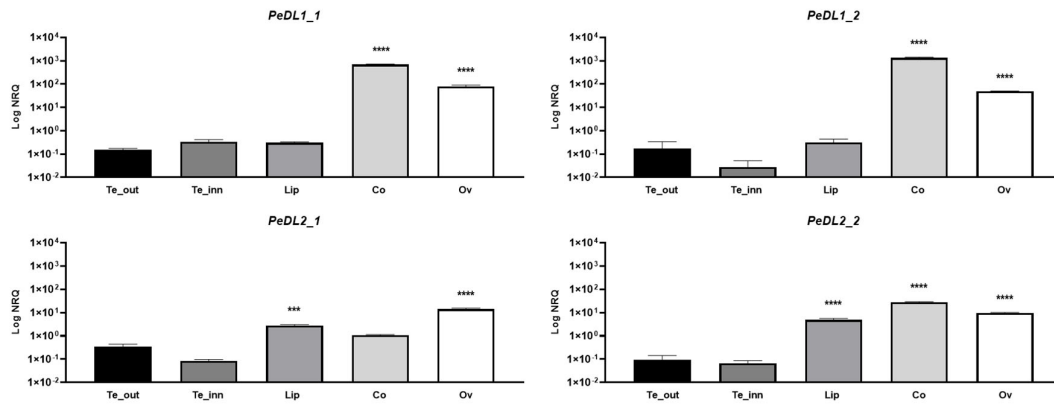


Figure 3. Relative expression of the different isoforms of the *PeDL1* and *PeDL2* genes in the floral tissues of the wild-type *Phalaenopsis* hyb. “Athens” at the B2 developmental stage (bud size 1–1.5 cm). The expression is reported as logarithm of the normalized relative quantity (Log NRQ). The bars represent the SEM of the biological and technical replicates. The asterisks indicate the statistically significant difference of the expression compared to outer tepals. p -Values *** < 0.001, **** < 0.0001. Te_out, outer tepals; Te_inn, lateral inner tepals; Co, column; Ov, ovary.

Then, to verify the conservation of these expression patterns and follow them along with flower development, we examined the expression profile of *PeDL1* and *PeDL2* in the perianth tissues of *P. aphrodite* at different developmental stages (Figure 1a,b). As shown in Figure 4, all but *PeDL2_1* have low expression levels in all the perianth organs (outer tepals, inner tepals, and labellum) from the earliest stage B1 to OF (open flower). Interestingly, the isoform *PeDL2_1* is expressed at high levels in the labellum during the first developmental stages. Its expression decreases over time, with a statistically significant negative correlation between expression level and stage (Spearman correlation $r = -1$, $p = 0.0028$).

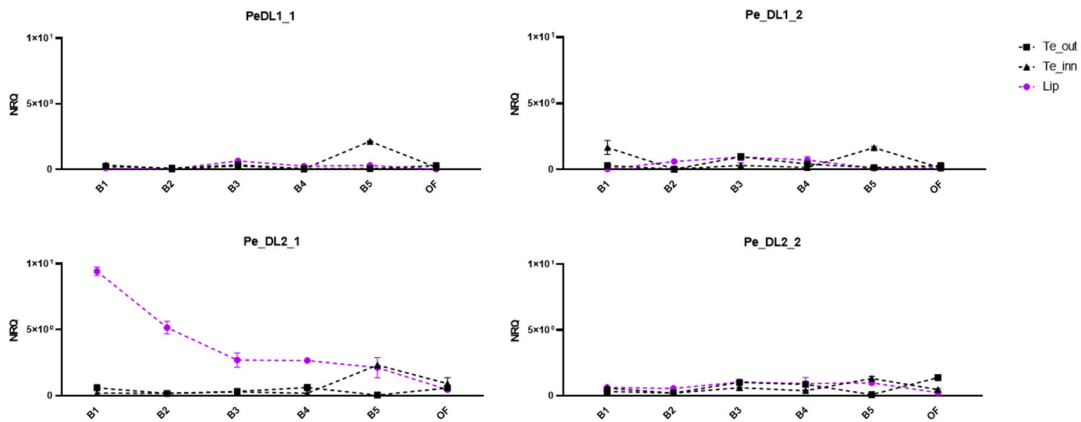


Figure 4. Relative expression of the different isoforms of the *PeDL1* and *PeDL2* genes in the perianth of the wild-type *P. aphrodite* at different developmental stages. The expression is reported as normalized relative quantity (NRQ). The bars represent the SEM of the biological and technical replicates. Bud size of the developmental stages: B1 (0.5–1 cm), B2 (1–1.5 cm), B3 (1.5–2 cm), B4 (2–2.5 cm), B5 (2.5–3 cm), OF (open flower). Te_out, outer tepals; Te_inn, lateral inner tepals.

To test the hypothesis that *PeDL2* is associated with the development of distinct perianth organs, we analyzed the expression pattern of the isoforms *PeDL2_1* and *PeDL2_2* in two *Phalaenopsis* peloric mutants bearing labellum-like structures in place of lateral inner tepals. The peloric *Phalaenopsis* hyb. “Athens” shows an increased expression of both *PeDL2* isoforms in the labellum-like structures compared to the lateral inner tepals of the

wild-type (Figure 5). In particular, the mean difference of the expression between lateral inner tepals and labellum decreases from -2.71 (wild-type) to -1.93 (peloric) for *PeDL2_1* and from -4.82 (wild-type) to -0.83 (peloric) for *PeDL2_2*. In the peloric *Phalaenopsis* hybrid “Joy Fairy Tale” there are no significant differences found in the expression levels of *PeDL2* in the inner and outer perianth organs (Figure 6). Additionally, no significant differences were detected in the expression of *PeDL1_1* and *PeDL1_2* in the perianth of wild-type and both peloric *Phalaenopsis* mutants (Supplementary Figure S3).

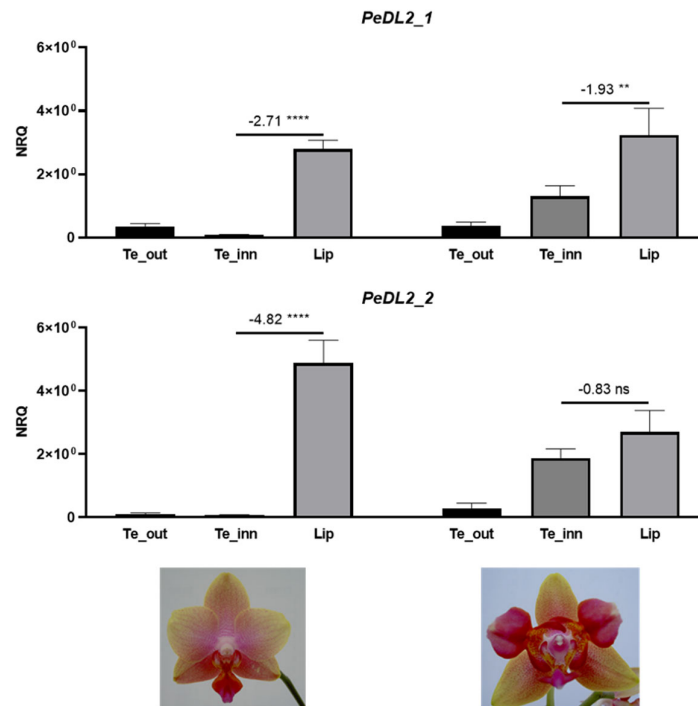


Figure 5. Relative expression of the isoforms *PeDL2_1* and *PeDL2_2* in the perianth of the wild-type and peloric *Phalaenopsis* hybrid “Joy Fairy Tale” at the 2. developmental stage (bud size 1–1.5 cm). The expression is reported as normalized relative quantity (NRQ). The vertical bars represent the SEM of the biological and technical replicates. The numbers above the horizontal lines are the mean differences of the expression between lateral inner tepals and labellum (Te_inn - Lip). *p*-Values ** < 0.01, **** < 0.0001; ns, not significant. Te_out, outer tepals; Te_inn, lateral inner tepals or labellum-like structures that substitute the lateral inner tepals in the peloric mutant.

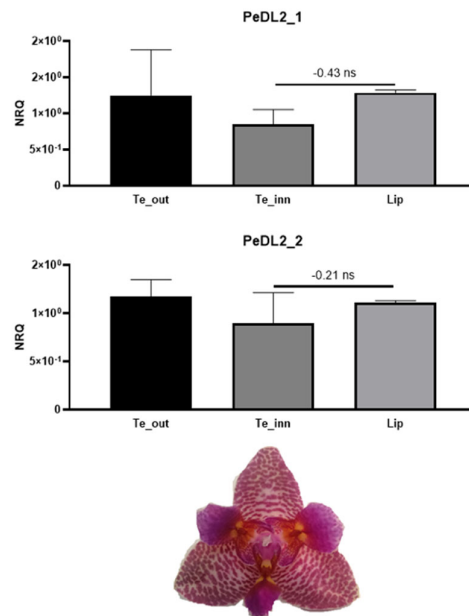


Figure 6. Relative expression of the isoforms *PeDL2_1* and *PeDL2_2* in the perianth of the peloric *Phalaenopsis* hybrid “Joy Fairy Tale” at the B2 developmental stage (bud size 1–1.5 cm). The expression is reported as normalized relative quantity (NRQ). The vertical bars represent the SEMs of the biological and technical replicates. The numbers above the horizontal lines are the mean differences of the expression between labellum-like structures and labellum (Te_{inn}-Lip). ns, not significant. Te_{out}, outer tepals; Te_{inn}, labellum-like structures that substitute the lateral inner tepals in the peloric mutant.

2.4. Differential Expression of the *PeMADS2*-*PeMADS5* Genes

To compare the expression profile of the *DEF*-like genes in the perianth organs of wild-type and peloric *Phalaenopsis*, we performed real-time PCR experiments on cDNA of wild-type and peloric *Phalaenopsis* hybrid “Athens” (Figure 7) and of the peloric *Phalaenopsis* hybrid “Joy Fairy Tale” (Figure 8). As expected, *PeMADS2* and *PeMADS5* are less expressed in labellum than in outer and inner tepals in the wild-type *Phalaenopsis*. Genes *PeMADS3* and *PeMADS4* show an opposite behavior, being more expressed in the labellum than in other organs of the wild-type perianth. In the peloric *Phalaenopsis* “Athens”, the mean difference between the expression levels of the *PeMADS2*-*PeMADS5* genes in labellum-like structures and labellum decreases due to the reduced (for *PeMADS2* and *PeMADS5*) or the increased (for *PeMADS3* and *PeMADS4*) expression in the labellum-like structures (Figure 7).

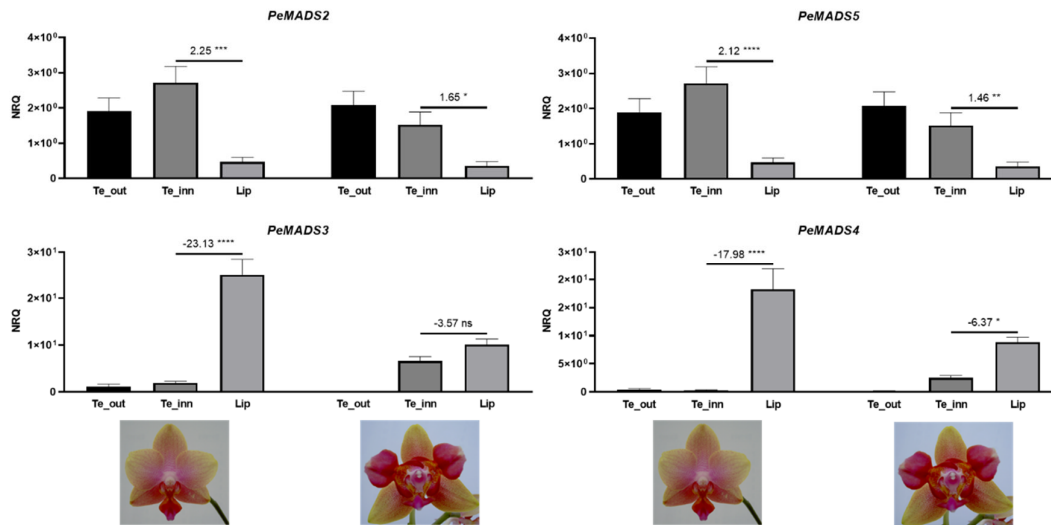


Figure 7. Relative expression of the class B MADS-box genes *PeMADS2*–*PeMADS5* in the perianth of *Phalaenopsis* hybrid “Athens” wild-type (left) and peloric mutant (right) at the B2 developmental stage (bud size 1–1.5 cm). The expression is reported as normalized relative quantity (NRQ). The vertical bars represent the SEM of the biological and technical replicates. The numbers above the horizontal lines are the mean differences of the expression between lateral inner tepals and labellum (Te_inn-Lip). *p*-Values * <0.05, ** <0.01, *** <0.001, **** <0.0001; ns, not significant. Te_out, outer tepals; Te_inn, lateral inner tepals or labellum-like structures that substitute the lateral inner tepals in the peloric mutant.

In the peloric *Phalaenopsis* hybrid “Joy Fairy Tale”, the differences in expression level between the labellum-like structures and lip are not significant, except for *PeMADS4*, which shows a higher expression in the labellum-like structures than in labellum (Figure 8).

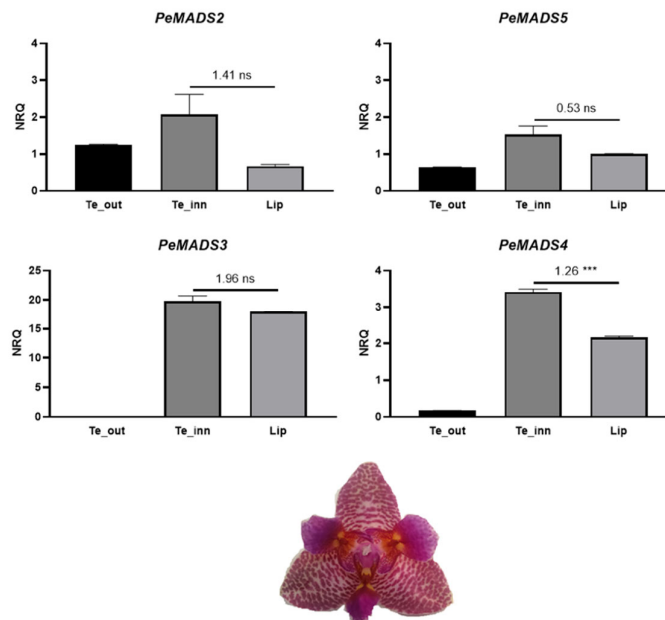


Figure 8. Relative expression of the class B MADS-box genes *PeMADS2*–*PeMADS5* in the perianth of *Phalaenopsis* hybrid “Joy Fairy Tale” at the B2 developmental stage (bud size 1–1.5 cm). The expression is reported as normalized relative quantity (NRQ). The vertical bars represent the SEM of the biological and technical replicates. The numbers above the horizontal lines are the mean differences of the expression between lateral inner tepals and labellum-like structures (Te_inn-Lip). *p*-Values *** <0.001; ns, not significant. Te_out, outer tepals; Te_inn, labellum-like structures that substitute the lateral inner tepals in the peloric mutant. Note the different scale for *PeMADS3*.

2.5. Protein Interaction: Y2H Analysis

We used the yeast two-hybrid (Y2H) assay to determine if the proteins PeMADS2-PeMADS5 and PeDL2_1 can interact (Supplementary Figure S4). Our results show that the DEF-like proteins of *Phalaenopsis* do not directly interact with PeDL2_1. We also checked the ability of PeDL2_1 to bind the GLO protein PeMADS6, equally expressed in all the perianth organs [14], also revealing the absence of direct interaction (Supplementary Figure S4). In addition, we verified the ability of both the isoforms of PeDL1 and PeDL2 to interact with each other, showing the absence of direct interaction in all the possible combinations (Supplementary Figure S4). As a positive control of the Y2H experiments, we tested the ability of PeMADS2-PeMADS5 to interact with PeMADS6. The results confirm that PeMADS6 can interact with each of the DEF-like proteins of *Phalaenopsis*, although with different strengths, as previously reported (Supplementary Figure S5) [46].

2.6. Conserved Regulatory Motifs

To search for conserved motifs within the promoters of the *PeDL* genes, we analyzed the 3000 bp upstream of the translation start site of the *DL2* genes of *Phalaenopsis equestris* (*PeDL2*) and *Dendrobium catenatum* (*DcDL2*). The MEME analysis revealed motifs shared by the putative promoters of *PeDL2* and *DcDL2* (Figure 9). Two motifs (Motifs 1 and 3) have a relatively well-conserved position within the ~300 bp upstream of the translation start site. These motifs were not found when the analysis was repeated using the shuffled sequences of the putative promoters (Supplementary Figure S6) and are not present within the putative promoter of the *DL1* gene (Supplementary Table S1).

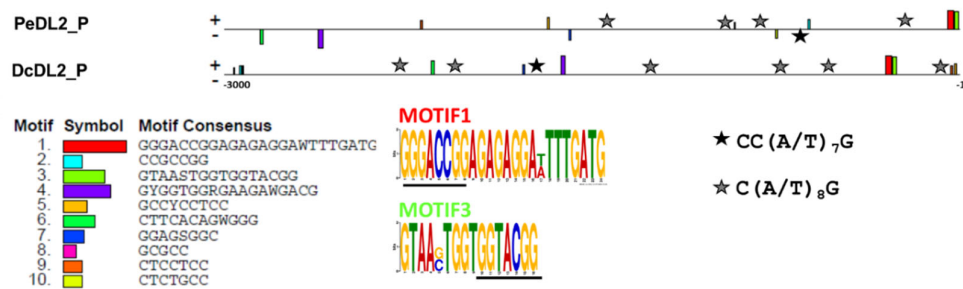


Figure 9. Conserved motifs within the putative promoters of the *DL2* genes of *P. equestris* and *D. catenatum*. *PeDL2_P* and *DcDL2_P* are the nucleotide sequences spanning 3000 bp upstream of the ATG translation start site, numbered from -1 to -3000 . In the sequence logo of Motifs 1 and 3, the predicted binding site of the TCP factor (JASPAR IDs MA1096.1 and MA1035.1) and of the SBP-type zinc finger (JASPAR ID MA0955.1) are underlined. The black and gray stars indicate the CArG-box variants $CC(A/T)_7G$ and $C(A/T)_8G$, respectively.

The TOMTOM analysis of Motif 1 against the JASPAR Core Plants database shows that it contains a putative binding site for a TCP protein. The same analysis conducted on Motif 3 revealed that it contains a putative binding site for an SBP-type zinc-finger protein (Figure 9).

The search of known transcription factor binding sites (TFBSs) within the putative promoters of the *DL2* genes of *Phalaenopsis* and *Dendrobium* through PLANTPAN 3.0 [47] identified putative conserved elements belonging to different transcription factor families. For example, in addition to the TCP and SBP binding sites, AP2/ERF, MYB/SANT, and MADS-box binding sites (CArG-boxes) were identified.

The specific search of CArG-boxes gave positive results for the variants $CC(A/T)_7G$ and $C(A/T)_8G$. In particular, one $CC(A/T)_7G$ site is present in both the *PeDL2* and *DcDL2* putative promoters. In addition, four and six $C(A/T)_8G$ sites are located within the *PeDL2*

and *DcDL2* promoters, respectively (Figure 9). One variant CC(A/T)₇G and four C(A/T)₈G CArG-boxes are also present within the putative promoter of *DcDL1*.

3. Discussion

Flower formation is the outcome of a complex developmental program in which environmental and genetic factors cooperate. The genetic pathway that drives the correct formation of the floral organs and the establishment of floral symmetry has been studied in detail in model species, where some transcription factor families play a relevant role, mainly MADS-box [11,12], TCP [21], MYB [29], and YABBY [38]. In orchids, the morphology of the flower organs and the establishment of bilateral floral symmetry have been widely studied, resulting in orchid-specific regulatory models where the coordinated action of MADS-box genes explains the formation of the orchid outer, lateral inner tepals, and labellum [13–19]. In the perspective of a broader, integrated view of these models, recent studies have suggested a possible involvement of TCP [26–28,35,48] and MYB [31,33] transcription factors in the developmental program leading to the formation of the orchid perianth, in particular of the labellum. In contrast, the possible involvement of the YABBY transcription factors in this developmental process is still unexplored. Based on these premises and the existence of a regulatory interaction between the YABBY transcription factor DL/CRC and the class B MADS domain transcription factors in rice (*OsMADS16*) [37,39] and maize (*silky*) [40], we tested the hypothesis of a similar regulatory relationship in orchids during the formation of the perianth organs, in particular of the labellum.

3.1. Paralogous DL-like Genes in Orchidaceae

Our results support the identification of two *DL*-like genes in the genome of *P. equestris*: *PeDL1* and *PeDL2* [49]. These genes belong to the CRABS CLAW/DROOPING LEAF clade. Each of them is part of one of the sister clades resulting from an Orchidaceae-specific duplication early after the divergence of subfamilies Apostasioideae and Vanilloideae (Supplementary Figure S7). Our results agree with the finding that *PeDL1* and *PeDL2* are expressed in the column and ovary of *Phalaenopsis* (Figure 3) [49]. This expression profile suggests that like in *Oryza*, *Zea*, *Triticum*, *Sorghum*, and *Arabidopsis*, *PeDL1* and *PeDL2* are also involved in carpel development [49–51].

3.2. Different Transcripts of DL-like Genes

We found two differentially spliced transcripts of the *PeDL1* and *PeDL2* genes of *Phalaenopsis*, differing at the 5' terminus (Figure 2) and encoding proteins completely (*PeDL1_2*) or partially (*PeDL2_2*) missing the C2C2 zinc-finger domain (Supplementary Figure S2). Although we scanned the transcriptomes of various orchid species present in the orchid-specific database Orchidstra 2.0 [52] and OrchidBase 2.0 [53], we did not find similar alternative short transcripts of the *DL* homolog genes. Our initial in silico identification of the *PeDL1_2* and *PeDL2_2* isoforms was verified by PCR, sequencing, and real-time PCR experiments using isoform-specific primers. Our results confirmed the existence of differentially spliced isoforms for both *PeDL* genes. The failure to find alternative transcripts of *DLs* in other orchids might be due to the kind of transcriptomes deposited in the orchid-specific database. This data generally represents transcripts of the whole inflorescence, with possible under-representation of isoforms expressed specifically in few types of cells or organs. Outside orchids, we found the annotation of two isoforms of both the *DL* genes of *Zea mays* *drl1* (https://maizegdb.org/gene_center/gene/GRMZM2G088309, access date 18 January 2021) and *drl2* (https://www.maizegdb.org/gene_center/gene/GRMZM2G102218, access date 18 January 2021). In particular, the predicted alternative isoform of the *drl2* gene encodes a short protein missing the C2C2 zinc-finger domain, as in *Phalaenopsis*. Unfortunately, functional or expression data for the *drl* isoforms are not available, and their role is still unknown. Further analyses are needed to

assess the function of the truncated isoforms that might work as competitive inhibitors and thus have a regulatory function.

In *Arabidopsis*, YABBY proteins form homo and heterodimers [54]. In particular, the CRC protein forms homodimers and can interact with the YABBY protein INO [55]. In contrast to CRC, our results indicate that PeDL1, PeDL2, and their short isoforms, form neither homo- nor heterodimers (Supplementary Figure S4), showing that the ability of CRC/DL proteins to homo- and heterodimerize is not conserved among plants. This unexpected result is in agreement with that reported in a recent study on the DL-like genes of *Phalaenopsis* [56] and might be due to sequence divergence after duplication, resulting in the loss of the ability to form homo- and heterodimers.

3.3. Divergent Patterns of Expression of PeDL1 and PeDL2 during Flower Development

Interestingly, the expression of the two *PeDL* genes in the perianth organs of wild-type *Phalaenopsis* is not overlapping. In contrast to very low expression levels of *PeDL1* in all perianth organs from early to late floral buds, *PeDL2* has a higher level of expression in the labellum than in outer and lateral inner tepals. This trend decreases steadily towards anthesis (Figure 3). Considering that the expression of *DL* in *O. sativa* is restricted to the flower meristem and developing carpels, the expression of *PeDL2* in the perianth is unusual for a *DL*-like gene, and is the first evidence of a possible novel regulatory function acquired by these genes after duplication early in orchid evolution. Our hypothesis of the recruitment of *PeDL2* in orchid perianth development is supported by the expression pattern of the gene in orchid peloric mutants where the inner tepals are substituted by labellum-like structures. In the peloric *Phalaenopsis* “Athens” (Figure 1d), early expression of both *PeDL2* isoforms increases in labellum-like inner lateral tepals compared to the wild type (Figure 5). In addition, the peloric *Phalaenopsis* “Joy Fairy Tale” (Figure 1e) shows similar expression of *PeDL2* in labellum-like structures and labellum (Figure 6). These results support the relationship between the combinatorial expression of *PeDL2*, *PeMADS3*, and *PeMADS4* transcripts and labellum development.

3.4. The “Orchid Code” beyond MADS

The idea of an “orchid code” enriched by the function of *PeDL2* during the labellum development fully fits with the regulatory profile of the other well-known components of this model: the *DEF*-like MADS-box genes *PeMADS2*–*PeMADS5*. In wild-type *Phalaenopsis*, the expression in the perianth of *PeDL2* has a similar pattern in the labellum and lateral outer tepals as *PeMADS3* and *PeMADS4* and is opposite to that of *PeMADS2* and *PeMADS5*.

The transcription patterns of *PeDL2* and *PeMADS2*–*PeMADS5* in wild-type and peloric *Phalaenopsis* allow us to suggest that during the formation of the labellum there could be regulatory interactions between *PeMADS2*–*PeMADS5* and *PeDL2*, based on different possible molecular mechanisms: either *PeMADS* proteins bind to regulatory DNA of the *PeDL2* gene (i.e., protein–DNA interactions), or *PeMADS* and *PeDL2* proteins interact (protein–protein interactions) (Figure 10). Although our results from the Y2H analysis do not reveal the ability of *PeDL2* to bind any of the *PeMADS2*–*PeMADS5* proteins, a direct protein–protein interaction cannot be definitely excluded, as it could require the formation of a multimeric protein complex.

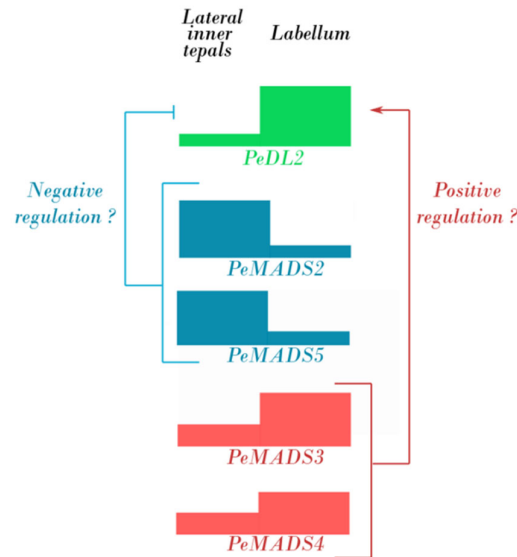


Figure 10. Possible regulatory interaction between *PeDL2* and *PeMADS2*–*PeMADS5* during the formation of the labellum of wild-type *Phalaenopsis*.

Alternatively, the regulatory interaction between *PeDL2* and *PeMADS2*–*PeMADS5* might be carried out at the transcriptional level, with *PeMADS2/5* functioning as transcriptional repressors or *PeMADS3/4* as transcriptional activators of the *PeDL2* gene. The MADS-box proteins are transcription factors that bind conserved sites on DNA with the consensus sequence CC(A/T)₆GG, the canonical CArG-box, or its variants [57]. The presence of the variant CArG-boxes CC(A/T)₇G and C(A/T)₈G (Figure 9), known transcription factor binding sites of MADS-domain proteins, in multiple sites of the putative promoter of *DL2* of *Phalaenopsis* and *Dendrobium* suggests that orchid DEF-like proteins or other MIKC-MADS domain genes could regulate the transcription of *DL2*. The presence of multiple CArG-boxes even strongly suggests that tetrameric complexes of MIKC-type proteins (“floral quartets”) are constituted [19,58]. In addition, the presence of shared transcription factor binding sites of TCP and SBP proteins, conserved in sequence and spatial organization in the putative promoters of *DL2*, suggests that other transcription factors could also modulate the expression of this gene to the expression domains here documented.

3.5. Conclusions

The molecular basis of orchid flower development is only partially understood. The main components of the orchid “toolkit for beauty” are MADS-box transcription factors; however, other transcription factor families (TCP and MYB) contribute to the differentiation of the organs of the orchid perianth. Our study proposes further expanding this complex developmental program, including the YABBY *PeDL2* of *Phalaenopsis* among the genes responsible for the labellum differentiation. Future studies should be focused on understanding the way of interaction among the different players of this fascinating developmental program to shed light on their regulatory connections.

4. Materials and Methods

4.1. Plant Material

The orchids used in this study were the wild-type *Phalaenopsis* hyb. “Athens” and *P. aphrodite* and the peloric mutants *Phalaenopsis* hyb. “Athens” and *Phalaenopsis* hyb. “Joy Fairy Tale”. All the plants were grown under natural light and temperature in the greenhouse of the Department of Biology (University of Naples Federico II, Napoli, Italy) or of

the Department of Cell Biology and Plant Biochemistry (University of Regensburg, Regensburg, Germany).

The wild-type *Phalaenopsis* has the second floral whorl clearly distinguished into two lateral inner tepals and one median inner tepal (labellum or lip) (Figure 1a–c). Both peloric mutants have two labellum-like organs in substitution of the lateral inner tepals (Figure 1d,e).

Single flowers from three different plants of the wild-type *P. aphrodite* were collected before anthesis at different developmental stages: B1 (bud length 0.5–1 cm), B2 (1–1.5 cm), B3 (1.5–2 cm), B4 (2–2.5 cm), and B5 (2.5–3 cm) (Figure 1a,b). Open flowers (OFs) were collected soon after anthesis (Figure 1a,b). Single flowers of six wild-type *Phalaenopsis* hyb. “Athens” and of the peloric mutants were collected at developmental stage B2.

The perianth tissues (outer tepals, lateral inner tepals, and labellum) of all the collected flowers at the different developmental stages as well as the column and ovary were dissected and immediately frozen in liquid nitrogen or immersed in RNAlater (Ambion, Austin, TX, USA) and stored at –80 °C until RNA extraction.

4.2. In Silico Identification of the *PeDL1* and *PeDL2* Genes

Total RNA was extracted from inner lateral tepals and labellum of wild-type and labellum-like lateral inner tepals from peloric *Phalaenopsis* hyb. “Athens” collected from 3 individual plants at the B2 developmental stage using Trizol (Ambion) followed by DNase treatment. After extraction, RNA was analyzed with the 2100 Bioanalyzer system (Agilent Technologies, Santa Clara, CA, USA) for sizing, quantitation, and quality control. Samples between 1 and 1.5 µg with an RIN (RNA integrity number) between 8.5 and 9.0 were sequenced by Macrogen (Seoul, Korea). Illumina TruSeq RNA (Oligo dT) mate paired-end libraries were generated and individually sequenced in a lane with a coverage >150 million 100 bp pair-end reads. For each sample 220 million paired-end reads were obtained. Analysis with FastQC showed that 94% of them had a quality score over 30. Trimming and mapping to the *Phalaenopsis equestris* genome v 1.0 (ASM126359v1) were carried out with the CLC Genomics Workbench (v11.01).

The Illumina raw reads of wild-type and peloric mutant *Phalaenopsis* hyb. “Brother Spring Dancer” KHM190 [59] were downloaded from the Sequence Read Archive. Paired-end reads from wild-type and peloric mutant outer tepal (accession numbers SRR1055198 and SRR1055947), inner tepal (SRR1055945 and SRR1055948), and labellum (SRR1055946 and SRR1055949) were assembled using the Trinity v2.3.0 software [60]. The Annocript v2.0.1 software [61] was used to obtain the functional annotation of the transcripts, and differential gene expression analysis between wild-type and peloric mutant tissues was performed with the edgeR v3.13 software [62].

The genomic organization of the *PeDL1* and *PeDL2* genes was reconstructed through BLAST analyses against the genome of *P. equestris* (assembly ASM126359v1), using as query the nucleotide sequence of the *DL*-like transcripts present in the transcriptome of *Phalaenopsis* hyb. “Brother Spring Dancer”.

4.3. Quantitative Expression Analysis

Total RNA was extracted from the tissues collected at the different developmental stages using Trizol (Ambion) followed by DNase treatment. After RNA extraction and quantification, equal amounts of total RNA were pooled, producing two pools for each tissue, each made of three different RNAs. Then, 500 ng of total RNA from each pool were reverse-transcribed using the Advantage RT-PCR kit (Clontech, Mountain View, CA, USA) and a mix of oligo dT and random hexamer primers.

The nucleotide sequences of the *PeDL1* and *PeDL2* transcripts and of their alternatively spliced isoforms identified by in silico analysis were verified through PCR amplification of the cDNA of *Phalaenopsis* hyb. “Athens” using gene- and isoform-specific primer pairs (Supplementary Table S2). The amplification products were cloned into pSC-A-amp/kan vector (Agilent Technologies, Santa Clara, CA, USA) and sequenced using the

T3 and T7 primers (Eurofins Genomics, Ebersberg, Germany). The nucleotide sequences were deposited in GenBank with the following accession numbers: MW574592 (*PeDL1_1*), MW574593 (*PeDL1_2*), MW574594 (*PeDL2_1*), MW574595 (*PeDL2_2*).

Relative expression of *PeDL1* (two isoforms: *PeDL1_1* and *PeDL1_2*), *PeDL2* (two isoforms: *PeDL2_1* and *PeDL2_2*), *PeMADS2*, *PeMADS5*, *PeMADS3*, and *PeMADS4* was evaluated in all the collected tissues by qPCR experiments, using 18S, *Actin*, and *Elongation Factor 1 α* as reference genes, as previously described [20]. The gene- and isoform-specific primer pairs used are listed in the Supplementary Table 2. At least one primer for each pair was constructed spanning two adjacent exons (Figure 2). The reactions were conducted in technical triplicates. Normalized relative quantity (NRQ) \pm SEM was calculated for each replicate to the geometric average expression of three internal control genes [20].

ANOVA analysis followed by Holm–Sidak post-hoc test was performed to assess the statistical significance of the differences of NRQ among the different tissues.

4.4. Yeast Two-Hybrid Analysis

The GAL4-based yeast two-hybrid (Y2H) system (Matchmaker two-hybrid system; Clontech) was used to analyze protein–protein interactions between *PeDL2_1* and *PeMADS2*–*PeMADS6*, and between the different isoforms of *PeDL1* and *PeDL2*. As positive control, Y2H analysis was used to check the ability of *PeMADS6* to form heterodimers with *PeMADS2*–*PeMADS5*.

The full-length coding regions of *PeDL1_1* (MW574592), *PeDL1_2* (MW574593), *PeDL2_1* (MW574594), *PeDL2_2* (MW574595), *PeMADS2* (AY378149), *PeMADS3* (AY378150), *PeMADS4* (AY378147), *PeMADS5* (AY378148), and *PeMADS6* (AY678299) were amplified by PCR using the primer pairs listed in Supplementary Table 2 and sub-cloned into the yeast expression vectors pGADT7 (prey) and pGBKT7 (bait) from the MATCHMAKER two-hybrid system 3 (Clontech), in frame with the sequence of either the transcription-activating (AD) or DNA-binding domains (BD) of the transcription factor GAL4. *Saccharomyces cerevisiae* strain AH109 was transformed with all the prey and bait recombinant vector combinations [63], conducting each experiment in triplicate.

Plasmid presence after double yeast transformations was verified by growing cells in Synthetic Defined (SD) medium lacking tryptophan and leucine. Protein–protein interaction was tested in SD medium lacking tryptophan, leucine, and histidine. Possible transcriptional activation activity of *PeDLs* and *PeMADS2*–*6* proteins fused to the binding domain of GAL4 (pGBKT7 vector) was checked by monitoring the growth of yeast transformed cells in SD medium without histidine, in the presence of 20 mM 3-aminotriazole (3AT). Empty vectors pGBKT7 or pGADT7 were transformed in combination with the recombinant vectors as negative controls.

4.5. Identification of Conserved Motifs

Nucleotide sequences (3000 bp) upstream of the *PeDL2* gene of *P. equestris* were downloaded, as were the 3000 bp upstream of the *DcDL2* and *DcDL1* of *D. catenatum*. Unfortunately, it was impossible to download the sequence upstream of the *PeDL1* gene because the genomic scaffold starts with the coding sequence of this gene.

Putative promoter sequences were scanned for the presence of conserved motifs using the online tool MEME v5.3.3 [64] with the following parameters: motif width between 5 and 25, one occurrence of motif per sequence, and the maximum number of motifs 10. The search was repeated with the same parameters on the shuffled sequences as negative control. The identified conserved motifs were then checked against the JASPAR2020 Core Plants database (<http://jaspar.genereg.net/>, access date 18 January 2021) through TOMTOM v5.3.3 [65].

The search of known transcription factor binding sites within the putative promoters was conducted in PLANTPAN 3.0 [47]. In addition, using the FUZZNUC software (<http://emboss.bioinformatics.nl/cgi-bin/emboss/fuzznuc>), the putative promoters were

scanned for the presence of perfect CARG-boxes CC(A/T)6GG and for the variants CC(A/T)7G and C(A/T)8G.

Supplementary Materials: Supplementary materials can be found at www.mdpi.com/article/10.3390/ijms22137025/s1. Figure S1. Transcripts expressed in perianth organs of wild-type (WT) and peloric *Phalaenopsis* hyb. “Athens” with at least 1 TPM. Figure S2. Amino acid alignment of the different isoforms of the PeDL1 and PeDL2 proteins of *P. equestris*. Figure S3. Relative expression of the isoforms *PeDL1_1* and *PeDL1_2* in the perianth of the wild-type (a) and peloric (b) *Phalaenopsis* hyb. “Athens” and of the peloric *Phalaenopsis* hyb. “Joy Fairy Tale” (c) at the B2 developmental stage (bud size 1–1.5 cm). Figure S4. Interactions of the PeDL2_1 and PeMADS2–6 (left) and the different isoforms of PeDL1/2 (right) of *Phalaenopsis* in yeast two-hybrid analysis. Figure S5. Interactions of PeMADS2–PeMADS5 and PeMADS6 of *Phalaenopsis* in yeast two-hybrid analysis. Figure S6. Conserved motifs within the shuffled sequences of the putative promoters of the *DL2* genes of *P. equestris* and *D. catenatum*. Figure S7. Neighbor joining tree of the CRC/DL proteins. Table S1. Conserved motifs of the putative promoters of the *PeDL2* and *DcDL2* genes found within the putative promoter of the *DcDL1* gene. Table S2. List of the primer sequences used. Data S1. Differentially expressed transcripts (FDR < 0.05) between lateral inner tepals and labellum of wild-type *Phalaenopsis* hyb. Data S2. Selected differentially expressed transcripts (FDR < 0.05) between labellum and inner tepals of wild-type and peloric *Phalaenopsis* hyb.

Author Contributions: Conceptualization, M.M.-P. and S.A.; methodology, F.L., M.C.V., and S.N.; validation, F.L. and M.C.V.; formal analysis, M.M.-P., S.A., G.T., S.N., F.L., and M.C.V.; writing—original draft preparation, M.M.-P. and S.A.; supervision, M.M.-P. and S.A.; funding acquisition, S.A. All authors have read and agreed to the published version of the manuscript.

Funding: This research was funded by Università degli Studi di Napoli Federico II, grant number 000020-2019.

Institutional Review Board Statement: Not applicable.

Informed Consent Statement: Not applicable.

Data Availability Statement: The data presented in this study are openly available in NCBI (<https://www.ncbi.nlm.nih.gov/>) with the following accession numbers: PeDL1_1 (MW574592), PeDL1_2 (MW574593), PeDL2_1 (MW574594), PeDL2_2 (MW574595), PeMADS2 (AY378149), PeMADS3 (AY378150), PeMADS4 (AY378147), PeMADS5 (AY378148), PeMADS6 (AY678299), *Phalaenopsis equestris* genome v 1.0 (ASM126359v1), reads from wild-type and peloric mutant outer tepal (accession numbers SRR1055198 and SRR1055947), *Phalaenopsis* hyb. “Brother Spring Dancer” KHM190 Illumina reads of inner tepal (SRR1055945, wild-type, and SRR1055948, peloric), and labellum (SRR1055946, wild-type, and SRR1055949, peloric).

Conflicts of Interest: The authors declare no conflicts of interest.

References

- Aceto, S.; Gaudio, L. The MADS and the Beauty: Genes Involved in the Development of Orchid Flowers. *Curr. Genom.* **2011**, *12*, 342–356, doi:10.2174/138920211796429754.
- Cozzolino, S.; Widmer, A. Orchid diversity: An evolutionary consequence of deception? *Trends Ecol. Evol.* **2005**, *20*, 487–494, doi:10.1016/j.tree.2005.06.004.
- Tremblay, R.L.; Ackerman, J.D.; Zimmerman, J.K.; Calvo, R.N. Variation in sexual reproduction in orchids and its evolutionary consequences: A spasmodic journey to diversification. *Biol. J. Linn. Soc.* **2005**, *84*, 1–54, doi:10.1111/j.1095-8312.2004.00400.x.
- Rudall, P.J.; Bateman, R.M. Roles of synorganisation, zygomorphy and heterotopy in floral evolution: The gynostemium and labellum of orchids and other lilioid monocots. *Biol. Rev.* **2002**, *77*, 403–441, doi:10.1017/S1464793102005936.
- Bateman, R.M.; Rudall, P.J. The good, the bad and the ugly: Using naturally occurring terata to distinguish the possible from the impossible in orchid floral evolution. In *Monocots: Comparative Biology and Evolution. Excluding Poales*; Columbus, J.T., Friar, E.A., Porter, J.M., Prince, L.M., Simpson, M.G., Eds.; Rancho Santa Ana Botanical Garden: Claremont, CA, USA, 2006; Volume I, pp. 481–496.
- Kocyan, A.; Endress, P.K. Floral structure and development and systematic aspects of some ‘lower’ Asparagales. *Plant Syst. Evol.* **2001**, *229*, 187–216, doi:10.1007/s006060170011.
- Burnsbalogh, P.; Bernhardt, P. Evolutionary Trends in the Androecium of the Orchidaceae. *Plant Syst. Evol.* **1985**, *149*, 119–134, doi:10.1007/Bf00984157.
- Darwin, C. *On the Various Contrivances by which British and Foreign Orchids Are Fertilised by Insects*; Murray: London, UK, 1862.
- Wordsell, W.C. *Principles of Plant Teratology*; The Ray Society: London, UK, 1916.

10. Endress, P.K. *Diversity and Evolutionary Biology of Tropical Flowers*; Cambridge University Press: Cambridge, UK, 1994.
11. Bowman, J.L.; Smyth, D.R.; Meyerowitz, E.M. Genetic Interactions among Floral Homeotic Genes of Arabidopsis. *Development* **1991**, *112*, 1–20.
12. Coen, E.S.; Meyerowitz, E.M. The War of the Whorls—Genetic Interactions Controlling Flower Development. *Nature* **1991**, *353*, 31–37, doi:10.1038/353031a0.
13. Mondragon-Palomino, M.; Theissen, G. Why are orchid flowers so diverse? Reduction of evolutionary constraints by paralogues of class B floral homeotic genes. *Ann. Bot.-Lond.* **2009**, *104*, 583–594, doi:10.1093/aob/mcn258.
14. Mondragon-Palomino, M.; Theissen, G. Conserved differential expression of paralogous DEFICIENS- and GLOBOSA-like MADS-box genes in the flowers of Orchidaceae: Refining the ‘orchid code’. *Plant J.* **2011**, *66*, 1008–1019, doi:10.1111/j.1365-313X.2011.04560.x.
15. Mondragon-Palomino, M.; Theissen, G. MADS about the evolution of orchid flowers. *Trends Plant Sci.* **2008**, *13*, 51–59, doi:10.1016/j.tplants.2007.11.007.
16. Pan, Z.J.; Cheng, C.C.; Tsai, W.C.; Chung, M.C.; Chen, W.H.; Hu, J.M.; Chen, H.H. The duplicated B-class MADS-box genes display dualistic characters in orchid floral organ identity and growth. *Plant Cell Physiol.* **2011**, *52*, 1515–1531, doi:10.1093/pcp/pcr092.
17. Chang, Y.Y.; Kao, N.H.; Li, J.Y.; Hsu, W.H.; Liang, Y.L.; Wu, J.W.; Yang, C.H. Characterization of the possible roles for B class MADS box genes in regulation of perianth formation in orchid. *Plant Physiol.* **2010**, *152*, 837–853, doi:10.1104/pp.109.147116.
18. Su, C.L.; Chen, W.C.; Lee, A.Y.; Chen, C.Y.; Chang, Y.C.; Chao, Y.T.; Shih, M.C. A modified ABCDE model of flowering in orchids based on gene expression profiling studies of the moth orchid *Phalaenopsis aphrodite*. *PLoS ONE* **2013**, *8*, e80462, doi:10.1371/journal.pone.0080462.
19. Hsu, H.F.; Hsu, W.H.; Lee, Y.I.; Mao, W.T.; Yang, J.Y.; Li, J.Y.; Yang, C.H. Model for perianth formation in orchids. *Nat. Plants* **2015**, *1*, doi:10.1038/Nplants.2015.46.
20. Acri-Nunes-Miranda, R.; Mondragón Palomino, M. Expression of paralogous *SEP*-, *FUL*-, *AG*- and *STK*-like MADS-box genes in wild-type and peloric *Phalaenopsis* flowers. *Front. Plant Sci.* **2014**, 1–17, doi:10.3389/fpls.2014.00076/abstract.
21. Luo, D.; Carpenter, R.; Copesey, L.; Vincent, C.; Clark, J.; Coen, E. Control of organ asymmetry in flowers of *Antirrhinum*. *Cell* **1999**, *99*, 367–376.
22. Feng, X.Z.; Zhao, Z.; Tian, Z.X.; Xu, S.L.; Luo, Y.H.; Cai, Z.G.; Wang, Y.M.; Yang, J.; Wang, Z.; Weng, L.; et al. Control of petal shape and floral zygomorphy in *Lotus japonicus*. *Proc. Natl. Acad. Sci. USA* **2006**, *103*, 4970–4975, doi:10.1073/pnas.0600681103.
23. Busch, A.; Zachgo, S. Control of corolla monosymmetry in the Brassicaceae *Iberis amara*. *Proc. Natl. Acad. Sci. USA* **2007**, *104*, 16714–16719, doi:10.1073/pnas.0705338104.
24. Broholm, S.K.; Tahtiharju, S.; Laitinen, R.A.E.; Albert, V.A.; Teeri, T.H.; Elomaa, P. A TCP domain transcription factor controls flower type specification along the radial axis of the *Gerbera* (Asteraceae) inflorescence. *Proc. Natl. Acad. Sci. USA* **2008**, *105*, 9117–9122, doi:10.1073/pnas.0801359105.
25. Zhang, W.H.; Kramer, E.M.; Davis, C.C. Floral symmetry genes and the origin and maintenance of zygomorphy in a plant-pollinator mutualism. *Proc. Natl. Acad. Sci. USA* **2010**, *107*, 6388–6393, doi:10.1073/pnas.0910155107.
26. De Paolo, S.; Gaudio, L.; Aceto, S. Analysis of the TCP genes expressed in the inflorescence of the orchid *Orchis italica*. *Sci. Rep.* **2015**, *5*, 16265, doi:10.1038/srep16265.
27. Lin, Y.F.; Chen, Y.Y.; Hsiao, Y.Y.; Shen, C.Y.; Hsu, J.L.; Yeh, C.M.; Mitsuda, N.; Ohme-Takagi, M.; Liu, Z.J.; Tsai, W.C. Genome-wide identification and characterization of TCP genes involved in ovule development of *Phalaenopsis equestris*. *J. Exp. Bot.* **2016**, *67*, 5051–5066, doi:10.1093/jxb/erw273.
28. Madrigal, Y.; Alzate, J.F.; Pabon-Mora, N. Evolution and Expression Patterns of TCP Genes in Asparagales. *Front. Plant Sci.* **2017**, *8*, doi:10.3389/fpls.2017.00009.
29. Raimundo, J.; Sobral, R.; Bailey, P.; Azevedo, H.; Galego, L.; Almeida, J.; Coen, E.; Costa, M.M.R. A subcellular tug of war involving three MYB-like proteins underlies a molecular antagonism in *Antirrhinum* flower asymmetry. *Plant J.* **2013**, *75*, 527–538.
30. Raimundo, J.; Sobral, R.; Laranjeira, S.; Costa, M.M.R. Successive Domain Rearrangements Underlie the Evolution of a Regulatory Module Controlled by a Small Interfering Peptide. *Mol. Biol. Evol.* **2018**, *35*, 2873–2885, doi:10.1093/molbev/msy178.
31. Valoroso, M.C.; De Paolo, S.; Iazzetti, G.; Aceto, S. Transcriptome-Wide Identification and Expression Analysis of DIVARICATA- and RADIALIS-Like Genes of the Mediterranean Orchid *Orchis italica*. *Genome Biol. Evol.* **2017**, *9*, doi:10.1093/gbe/evx101.
32. Lucibelli, F.; Valoroso, M.C.; Aceto, S. Radial or Bilateral? The Molecular Basis of Floral Symmetry. *Genes-Basel* **2020**, *11*, doi:10.3390/Genes11040395.
33. Valoroso, M.C.; Sobral, R.; Saccone, G.; Salvemini, M.; Costa, M.M.R.; Aceto, S. Evolutionary Conservation of the Orchid MYB Transcription Factors DIV, RAD, and DRIF. *Front. Plant Sci.* **2019**, *10*, doi:10.3389/fpls.2019.01359.
34. Costa, M.M.R.; Fox, S.; Hanna, A.I.; Baxter, C.; Coen, E. Evolution of regulatory interactions controlling floral asymmetry. *Development* **2005**, *132*, 5093–5101.
35. Mondragon-Palomino, M.; Trontin, C. High time for a roll call: Gene duplication and phylogenetic relationships of TCP-like genes in monocots. *Ann. Bot.* **2011**, *107*, 1533–1544, doi:10.1093/aob/mcr059.

36. Nakayama, H.; Yamaguchi, T.; Tsukaya, H. Expression patterns of AaDL, a CRABS CLAW ortholog in *Asparagus asparagoides* (Asparagaceae), demonstrate a stepwise evolution of CRC/DL subfamily of YABBY genes. *Am. J. Bot.* **2010**, *97*, 591–600, doi:10.3732/ajb.0900378.
37. Yamaguchi, T.; Nagasawa, N.; Kawasaki, S.; Matsuoka, M.; Nagato, Y.; Hirano, H.Y. The YABBY gene DROOPING LEAF regulates carpel specification and midrib development in *Oryza sativa*. *Plant Cell* **2004**, *16*, 500–509, doi:10.1105/tpc.018044.
38. Sawa, S.; Ito, T.; Shimura, Y.; Okada, K. FILAMENTOUS FLOWER controls the formation and development of Arabidopsis inflorescences and floral meristems. *Plant Cell* **1999**, *11*, 69–86, doi:10.1105/tpc.11.1.69.
39. Nagasawa, N.; Miyoshi, M.; Sano, Y.; Satoh, H.; Hirano, H.; Sakai, H.; Nagato, Y. SUPERWOMAN1 and DROOPING LEAF genes control floral organ identity in rice. *Development* **2003**, *130*, 705–718, doi:10.1242/dev.00294.
40. Strable, J.; Vollbrecht, E. Maize YABBY genes drooping leaf1 and drooping leaf2 regulate floret development and floral meristem determinacy. *Development* **2019**, *146*, doi:10.1242/dev.171181.
41. Cantone, C.; Gaudio, L.; Aceto, S. The PI/GLO-like locus in orchids: Duplication and purifying selection at synonymous sites within Orchidinae (Orchidaceae). *Gene* **2011**, *481*, 48–55, doi:10.1016/j.gene.2011.04.004.
42. Cantone, C.; Sica, M.; Gaudio, L.; Aceto, S. The OrcPI locus: Genomic organization, expression pattern, and noncoding regions variability in *Orchis italica* (Orchidaceae) and related species. *Gene* **2009**, *434*, 9–15, doi:10.1016/j.gene.2008.12.015.
43. Cai, J.; Liu, X.; Vanneste, K.; Proost, S.; Tsai, W.C.; Liu, K.W.; Chen, L.J.; He, Y.; Xu, Q.; Bian, C.; et al. The genome sequence of the orchid *Phalaenopsis equestris*. *Nat. Genet.* **2015**, *47*, 65–72, doi:10.1038/ng.3149.
44. Huang, J.Z.; Lin, C.P.; Cheng, T.C.; Chang, B.C.H.; Cheng, S.Y.; Chen, Y.W.; Lee, C.Y.; Chin, S.W.; Chen, F.C. A De Novo Floral Transcriptome Reveals Clues into *Phalaenopsis* Orchid Flower Development. *PLoS ONE* **2015**, *10*, doi:10.1371/journal.pone.0123474.
45. Tsai, W.C.; Kuoh, C.S.; Chuang, M.H.; Chen, W.H.; Chen, H.H. Four DEF-like MADS box genes displayed distinct floral morphogenetic roles in *Phalaenopsis* orchid. *Plant Cell Physiol.* **2004**, *45*, 831–844, doi:10.1093/pcp/pch095.
46. Tsai, W.C.; Pan, Z.J.; Hsiao, Y.Y.; Jeng, M.F.; Wu, T.F.; Chen, W.H.; Chen, H.H. Interactions of B-class complex proteins involved in tepal development in *Phalaenopsis* orchid. *Plant Cell Physiol.* **2008**, *49*, 814–824, doi:10.1093/pcp/pcn059.
47. Chow, C.N.; Lee, T.Y.; Hung, Y.C.; Li, G.Z.; Tseng, K.C.; Liu, Y.H.; Kuo, P.L.; Zheng, H.Q.; Chang, W.C. PlantPAN3.0: A new and updated resource for reconstructing transcriptional regulatory networks from ChIP-seq experiments in plants. *Nucleic Acids Res.* **2019**, *47*, D1155–D1163, doi:10.1093/nar/gky1081.
48. Chen, Y.H.; Tsai, Y.J.; Huang, J.Z.; Chen, F.C. Transcription analysis of peloric mutants of *Phalaenopsis* orchids derived from tissue culture. *Cell Res.* **2005**, *15*, 639–657, doi:10.1038/sj.cr.7290334.
49. Chen, Y.Y.; Hsiao, Y.Y.; Chang, S.B.; Zhang, D.; Lan, S.R.; Liu, Z.J.; Tsai, W.C. Genome-Wide Identification of YABBY Genes in Orchidaceae and Their Expression Patterns in *Phalaenopsis* Orchid. *Genes* **2020**, *11*, doi:10.3390/genes11090955.
50. Ishikawa, M.; Ohmori, Y.; Tanaka, W.; Hirabayashi, C.; Murai, K.; Ogihara, Y.; Yamaguchi, T.; Hirano, H.Y. The spatial expression patterns of DROOPING LEAF orthologs suggest a conserved function in grasses. *Genes Genet. Syst.* **2009**, *84*, 137–146, doi:10.1266/ggs.84.137.
51. Alvarez, J.; Smyth, D.R. CRABS CLAW and SPATULA, two Arabidopsis genes that control carpel development in parallel with AGAMOUS. *Development* **1999**, *126*, 2377–2386.
52. Chao, Y.T.; Yen, S.H.; Yeh, J.H.; Chen, W.C.; Shih, M.C. Orchidstra 2.0—A Transcriptomics Resource for the Orchid Family. *Plant Cell Physiol.* **2017**, *58*, doi:10.1093/pcp/pcw220.
53. Tsai, W.C.; Fu, C.H.; Hsiao, Y.Y.; Huang, Y.M.; Chen, L.J.; Wang, M.; Liu, Z.J.; Chen, H.H. OrchidBase 2.0: Comprehensive collection of Orchidaceae floral transcriptomes. *Plant Cell Physiol.* **2013**, *54*, e7, doi:10.1093/pcp/pcs187.
54. Stahle, M.I.; Kuehlich, J.; Staron, L.; von Arnim, A.G.; Golz, J.F. YABBYs and the transcriptional corepressors LEUNIG and LEUNIG_HOMOLOG maintain leaf polarity and meristem activity in Arabidopsis. *Plant Cell* **2009**, *21*, 3105–3118, doi:10.1105/tpc.109.070458.
55. Gross, T.; Broholm, S.; Becker, A. CRABS CLAW Acts as a Bifunctional Transcription Factor in Flower Development. *Front. Plant Sci.* **2018**, *9*, 835, doi:10.3389/fpls.2018.00835.
56. Chen, Y.Y.; Hsiao, Y.Y.; Li, C.I.; Yeh, C.M.; Mitsuda, N.; Yang, H.X.; Chiu, C.C.; Chang, S.B.; Liu, Z.J.; Tsai, W.C. The ancestral duplicated DL/CRC orthologs, PeDL1 and PeDL2, function in orchid reproductive organ innovation. *J. Exp. Bot.* **2021**, doi:10.1093/jxb/erab195.
57. Aerts, N.; de Bruijn, S.; van Mourik, H.; Angenent, G.C.; van Dijk, A.D.J. Comparative analysis of binding patterns of MADS-domain proteins in Arabidopsis thaliana. *BMC Plant Biol.* **2018**, *18*, 131, doi:10.1186/s12870-018-1348-8.
58. Theissen, G.; Melzer, R.; Rumpfer, F. MADS-domain transcription factors and the floral quartet model of flower development: Linking plant development and evolution. *Development* **2016**, *143*, 3259–3271, doi:10.1242/dev.134080.
59. Lee, C.Y.; Viswanath, K.K.; Huang, J.Z.; Lee, C.P.; Lin, C.P.; Cheng, T.C.; Chang, B.C.; Chin, S.W.; Chen, F.C. PhalDB: A comprehensive database for molecular mining of the *Phalaenopsis* genome, transcriptome and miRNome. *Genet. Mol. Res.* **2018**, *17*, gmr18051, doi:10.4238/gmr18051.
60. Grabherr, M.G.; Haas, B.J.; Yassour, M.; Levin, J.Z.; Thompson, D.A.; Amit, I.; Adiconis, X.; Fan, L.; Raychowdhury, R.; Zeng, Q.; et al. Full-length transcriptome assembly from RNA-Seq data without a reference genome. *Nat. Biotechnol.* **2011**, *29*, 644–652, doi:10.1038/nbt.1883.

61. Musacchia, F.; Basu, S.; Petrosino, G.; Salvemini, M.; Sanges, R. Annocript: A flexible pipeline for the annotation of transcriptomes able to identify putative long noncoding RNAs. *Bioinformatics* **2015**, *31*, 2199–2201, doi:10.1093/bioinformatics/btv106.
62. Robinson, M.D.; McCarthy, D.J.; Smyth, G.K. edgeR: A Bioconductor package for differential expression analysis of digital gene expression data. *Bioinformatics* **2010**, *26*, 139–140, doi:10.1093/bioinformatics/btp616.
63. Gietz, R.D.; Schiestl, R.H.; Willems, A.R.; Woods, R.A. Studies on the Transformation of Intact Yeast-Cells by the Liac/S-DNA/Peg Procedure. *Yeast* **1995**, *11*, 355–360.
64. Bailey, T.L.; Boden, M.; Buske, F.A.; Frith, M.; Grant, C.E.; Clementi, L.; Ren, J.Y.; Li, W.W.; Noble, W.S. MEME SUITE: Tools for motif discovery and searching. *Nucleic Acids Res.* **2009**, *37*, W202–W208, doi:10.1093/nar/gkp335.
65. Gupta, S.; Stamatoyannopoulos, J.A.; Bailey, T.L.; Noble, W.S. Quantifying similarity between motifs. *Genome Biol.* **2007**, *8*, doi:10.1186/Gb-2007-8-2-R24.